Jpn. J. Appl. Phys. Vol. 36 (1997) pp. 3569–3575
Part 1, No. 6A, June 1997

A Simple Graphical Method for Evaluating the Polarization and Relaxation Times of Dipoles or Densities and Energy Levels of Traps in a Dielectric Film from Transient Discharge Current

Hideharu MATSUURA*

Department of Electronics, Osaka Electro-Communication University, 18-8 Hatsu-cho, Neyagawa, Osaka 572, Japan

(Received January 6, 1997; accepted for publication March 24, 1997)

The purpose of this study is to propose a simple graphical method for determining the polarization and relaxation times of dipoles and for determining the densities and energy levels of traps in a dielectric film. Using the transient discharge current density $J_{\rm dis}(t)$ which flows in a capacitor consisting of a dielectric film between two electrodes, a function $S(t)$ is defined as $S(t) \equiv t \cdot J_{\rm dis}(t) \exp(1)$. For dipoles with discrete relaxation times (τ_i) or for traps with discrete energy levels (ΔE_{ti}) where the subscript i represents the i-th dipole or trap, $S(t)$ has peaks corresponding to each τ_i or ΔE_{ti}. Using each peak, therefore, one can easily determine the dipole polarization (P_{si}) and τ_i, or the trap density (N_{ti}) and ΔE_{ti}. By a simple curve-fitting procedure, moreover, one can easily evaluate the continuously distributed dipole polarization $P_{\rm s}(\tau)$ or energetically distributed trap density $N_{\rm t}(\Delta E_{\rm t})$.

KEYWORDS: dielectric, ferroelectric, insulator, polarization, trap, gate insulator of FET

1. Introduction

Dioxide silicon (SiO_2) has played an important role in the performance characteristics of large scale integrated circuits (LSIs). In order to enlarge the capacitance of the capacity in memory element cells in a dynamic random-access memory (DRAM) or to reduce the operating voltage of field-effect transistors (FETs), it is necessary to decrease the thickness of SiO_2, or to make use of insulators with dielectric constants higher than the dielectric constant (3.9) of SiO_2.

The dielectric breakdown of insulators is one of the most important problems affecting their reliability. Traps in insulators are reported to be one cause of this problem.[1] Moreover, an increase in leakage current at low electric fields, which could result in insulator breakdown, is induced by high-field stress, and may be related to the generation of traps in insulators.[2] Therefore, it is necessary to evaluate the densities and energy levels of traps in insulators.

There are transient capacitance methods for determining the densities and energy levels of traps, for example, deep level transient spectroscopy (DLTS)[3] and isothermal capacitance transient spectroscopy (ICTS)[4,5] for low-resistivity semiconductors, and the heterojunction-monitored capacitance (HMC) method[6,7] for high-resistivity semiconductors such as undoped hydrogenated amorphous silicon whose resistivity is about $10^9\,\Omega\cdot$cm. In the case of applying the transient capacitance methods to metal-insulator-semiconductor (MIS) diodes, mainly traps at the insulator/semiconductor interface can be investigated.[8,9]

Although the following methods can be applied to the evaluation of the densities and energy levels of traps in insulators, these methods are less tested than those for semiconductors. Photocurrent spectroscopic techniques[10] are suitable for evaluating the energy levels of deep traps around the mid gap, and charge-centroid methods[11,12] are suitable for evaluating the densities of the deep traps. Although the thermally stimulated current (TSC) method[13] is suitable for evaluating single-level shallow traps which could be related to current flow in insulators, the heating rate of samples should be kept rigidly constant during measurement. Moreover, in the case of emission processes different from thermal emission processes, it is difficult to analyze the data obtained using the TSC method. When the emission process in the film is unknown, an isothermal measurement is more suitable for evaluating the densities and energy levels of traps in insulators than the TSC method. Therefore, we have proposed the discharge current transient spectroscopy (DCTS) method in which the transient discharge current is isothermally measured in a capacitor consisting of an insulator film between two electrodes.[14,15] This method can be used to evaluate the densities and energy levels of not only single-level but also energetically distributed shallow traps ($< 1\,$eV).

When dielectrics (i.e., insulators with high dielectric constants) are used in DRAM, the device performance is sensitive to dipole polarization in dielectrics. Recently, a ferroelectric random-access memory, in which one memory element cell comprises one FET and one capacitor composed of a ferroelectric, has been investigated. Moreover, a metal-ferroelectric-semiconductor FET (MFSFET), in which the gate insulator is composed of a ferroelectric, has been attractive, because one memory element cell comprises the only FET. In order to make use of dielectrics or ferroelectrics as insulators in these devices, the densities and energy levels of traps in these materials should be investigated. Moreover, an understanding of the mechanism of dipole relaxation in these materials is essential.

In order to evaluate the dipole relaxation in these materials, there are the thermally stimulated depolarization current (TSDC) method and similar methods.[16–20] However, these methods require not only a rigid constant heating rate but also an assumed temperature dependence of the dipole relaxation time (τ). Therefore, an

*E-mail address: matsuura@isc.osakac.ac.jp

isothermal measurement is suitable for evaluating τ in dielectrics. DCTS is suitable for evaluating τ,[21,22] since the transient discharge current is measured isothermally in a capacitor consisting of a dielectric or ferroelectric film between two electrodes.

When an expression of the form $ax\exp(-ax)$ or $x\exp(-ax)$ is obtained where a is a parameter and x is a variable, the function is maximum at $x = 1/a$. In the case of $ax\exp(-ax)$, the maximum value is $\exp(-1)$. This concept is incorporated in the ICTS,[4,5] HMC,[6,7] and DCTS methods.[14,15,21,22] Moreover, this concept is applied to a graphical method for determining the densities and energy levels of impurities in a semiconductor from the temperature dependence of majority-carrier concentration.[23–25]

The purpose of this study is to combine two methods for determining the densities and energy levels of traps and for determining the polarization and relaxation times of dipoles using the transient discharge current of the capacitor which consists of an insulator, or dielectric or ferroelectric film between two electrodes. In the following section, we discuss how to analyze the transient discharge current density, and then discuss individual cases.

2. Analysis of Transient Discharge Current

2.1 *Theoretical consideration*

A capacitor, consisting of an insulator, or dielectric or ferroelectric film between two electrodes of unit area, is considered. When a voltage V_{cha} is applied to the capacitor in the interval of $-t_{cha} < t < 0$, a charge current density $J_{cha}(t)$ flows through the capacitor as shown in Fig. 1, where $J_{cha}(t)$ is the sum of the current density $J_c(t)$ for charging geometric capacity, the absorption current density $J_a(t)$, and the leakage current density $J_l(t)$ which flows over the film. $J_a(t)$ results from the capture of charges at traps and/or from the polarization of dipoles. At $t = 0$, the applied voltage is changed from V_{cha} to V_{dis}, where V_{dis} is the voltage at which the transient discharge current is measured. $J_l(t)$ should be much smaller than the other current densities at V_{dis}. Therefore, V_{dis} is usually zero. Since the resistance in the external circuit is very low, the charge due to the geometric capacity disappears in a short time. At $t \geq 0$, therefore, a discharge current density, which can be experimentally measured, arises due to the emission of charges at traps and/or from the depolarization of dipoles.

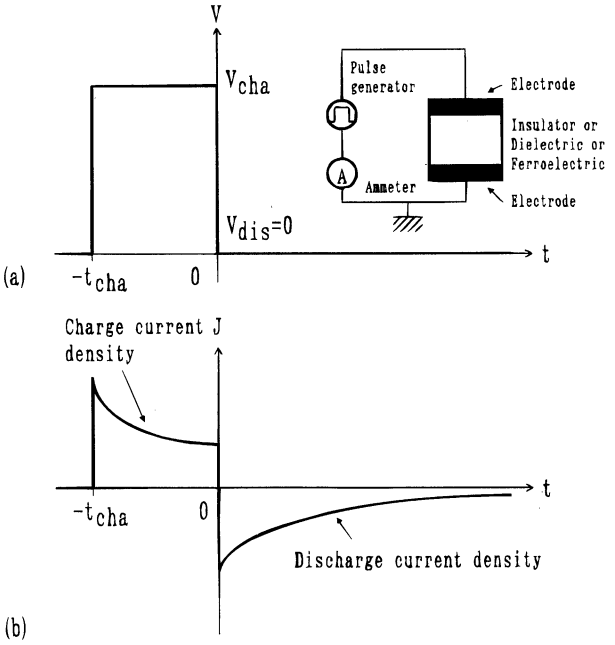

Fig. 1. Schematic representation of (a) voltage and (b) current density profiles. The circuit for a measurement of transient discharge current density is included.

2.1.1 *Discrete time constants*

Since the time dependence of the carrier emission from the i-th trap or the depolarization of the i-th dipole is given by

$$\exp\left(-\frac{t}{\tau_i}\right), \tag{1}$$

the total charge or the total polarization in the film of unit area, which is expressed as $Q(t)$, is given by

$$Q(t) = \sum_i F_i \exp\left(-\frac{t}{\tau_i}\right), \tag{2}$$

where τ_i is the time constant of the i-th trap or dipole, and F_i is the charge or the polarization in the film of unit area at $t = 0$, corresponding to τ_i. The absolute value $J_{dis}(t)$ of the transient discharge current density is given by

$$J_{dis}(t) = -\frac{dQ(t)}{dt} = \sum_i F_i \frac{1}{\tau_i} \exp\left(-\frac{t}{\tau_i}\right), \tag{3}$$

because the decrease of $Q(t)$ results in $J_{dis}(t)$. We define a function $S(t)$ as

$$S(t) \equiv t \cdot J_{dis}(t)\exp(1), \tag{4}$$

which is theoretically expressed as

$$S(t) = \sum_i F_i \exp(1)\frac{t}{\tau_i} \exp\left(-\frac{t}{\tau_i}\right). \tag{5}$$

As is clear from eq. (5), we have obtained a desirable function, because $S(t)$ includes the expression of the form; $(t/\tau_i)\exp(-t/\tau_i)$. Using the time (t_{peaki}) at which $S(t)$ exhibits the i-th peak, the values of τ_i and F_i can be determined as

$$\tau_i = t_{peaki} \tag{6}$$

and

$$F_i = S(t_{peaki}). \tag{7}$$

2.1.2 *Continuously distributed time constant*

In the case of continuously distributed τ, $Q(t)$ is given by

$$Q(t) = \int F(\tau)\exp\left(-\frac{t}{\tau}\right) d\tau, \tag{8}$$

where $F(\tau)$ is the charge or the polarization in the film of unit area at $t = 0$. $J_{dis}(t)$ is given by

$$J_{dis}(t) = -\frac{dQ(t)}{dt} = \int F(\tau)\frac{1}{\tau}\exp\left(-\frac{t}{\tau}\right) d\tau. \tag{9}$$

From eq. (4), $S(t)$ is expressed as

$$S(t) = \int F(\tau) \exp(1) \frac{t}{\tau} \exp\left(-\frac{t}{\tau}\right) d\tau. \quad (10)$$

As is clear from eq. (10), we have obtained a desirable function, because $S(t)$ includes the expression of the form; $(t/\tau)\exp(-t/\tau)$.

Let us discuss how to evaluate $F(\tau)$ using $S(t)$, based on the curve-fitting procedure incorporated in the HMC method which is used to evaluate the density-of-state distribution in the band gap of amorphous semiconductors.[6,7]

The value of $S(t)$ is calculated using $J_{dis}(t)$ and eq. (4). Using the first trial function $F^{(0)}(\tau)$ which is equal to the value of $S(t)$ at $t = \tau$, $S^{(0)}(t)$ is calculated using eq. (10). Since the function

$$\frac{t}{\tau} \exp\left(-\frac{t}{\tau}\right) \quad (11)$$

in eq. (10) has a maximum at $t = \tau$, $F^{(n-1)}(\tau)$ has the greatest influence on $S^{(n-1)}(t)$ at $t = \tau$, where n is an integer and $n \geq 1$. Therefore, the next trial function $F^{(n)}(\tau)$ is given by

$$F^{(n)}(\tau) = \frac{S(\tau)}{S^{(n-1)}(\tau)} F^{(n-1)}(\tau). \quad (12)$$

When $S^{(n)}(t)$ approaches $S(t)$ closely, we obtain the solution

$$F(\tau) = F^{(n)}(\tau). \quad (13)$$

2.2 Examples of the analysis of $J_{dis}(t)$

In order to demonstrate how to analyze $J_{dis}(t)$, three kinds of $J_{dis}(t)$ shown in Fig. 2 are considered. The solid curve represents $J_{dis}(t)$ for a constant $F(\tau)$ of 5×10^{-6} C/cm^2/log$_{10}$ s,[26] which is shown as the solid curve in Fig. 3. The broken curve represents $J_{dis}(t)$ for $F(\tau)$ shown as the broken curve in Fig. 3. The dashed-dotted curve represents $J_{dis}(t)$ for the film with three kinds of discrete F_i; $[\tau_i\ (s),\ F_i\ (\mathrm{C/cm^2})] = (0.3,\ 1 \times 10^{-5})$, $(10,\ 1 \times 10^{-5})$ and $(300,\ 1 \times 10^{-5})$.

The solid, broken and dashed-dotted curves in Fig. 4 represent $S(t)$ calculated using eq. (4) and $J_{dis}(t)$ expressed as the solid, broken and dashed-dotted curves in Fig. 2, respectively. In this figure, the dashed-dotted curve has three narrow peaks corresponding to the three kinds of discrete F_i, while the solid curve is nearly constant over the whole range, and the broken curve has two broad peaks.

Let us evaluate $F(\tau)$ using eq. (12) and $S(t)$ shown in Fig. 4.[27] The solid curve in Fig. 5 represents $F^{(n)}(\tau)$ for which $S^{(n)}(t)$ approaches $S(t)$ very closely. $F^{(n)}(\tau)$ is around 5×10^{-6} C/cm^2/log$_{10}$ s, which is close to $F(\tau)$ represented by the solid curve in Fig. 3. The broken curve in Fig. 5 represents $F^{(n)}(\tau)$ for which $S^{(n)}(t)$ approaches $S(t)$ very closely, and this broken curve is similar to the actual $F(\tau)$ shown by the broken curve in Fig. 3.

The dashed-dotted curve in Fig. 5 represents $F^{(n)}(\tau)$

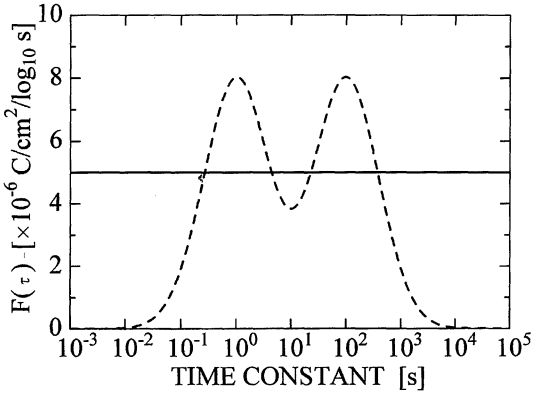

Fig. 3. Set of two kinds of $F(\tau)$ with continuously distributed τ, using which $J_{dis}(t)$ in Fig. 2 is calculated.

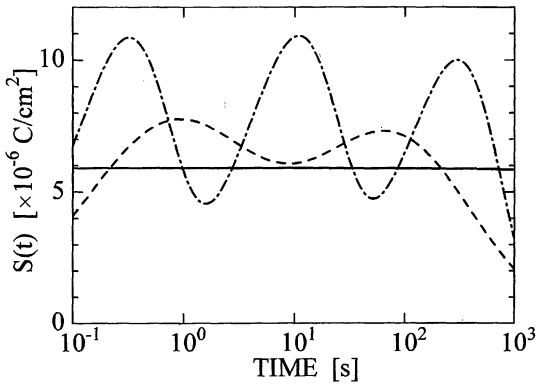

Fig. 4. $S(t)$ calculated using $J_{dis}(t)$ in Fig. 2.

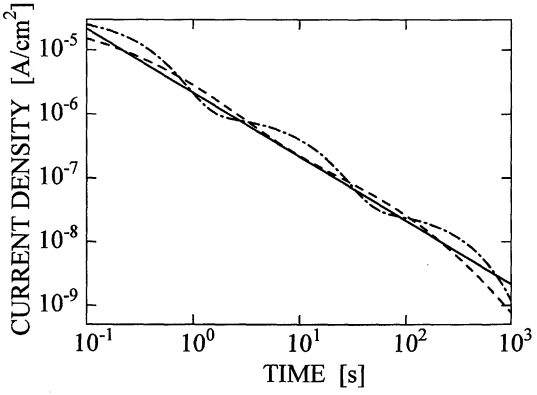

Fig. 2. Set of three kinds of $J_{dis}(t)$.

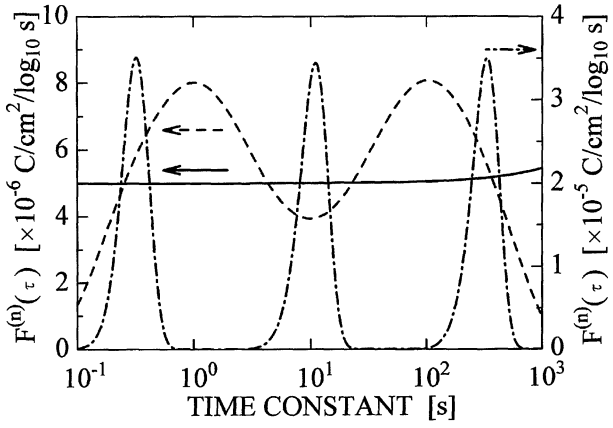

Fig. 5. $F^{(n)}(\tau)$ for which $S^{(n)}(t)$ approaches $S(t)$ shown in Fig. 4.

corresponding to the film with the three kinds of discrete F_i. Figure 6 shows $S(t)$ (solid curve) and $S^{(n)}(t)$ (broken curve) calculated using $F^{(n)}(\tau)$ shown by the dashed-dotted curve in Fig. 5. $S^{(n)}(t)$ is slightly different from $S(t)$, although we tried to obtain a value of $S^{(n)}(t)$ as close as possible to that of $S(t)$ using eq. (12). This case is quite different from the cases of $F(\tau)$ with continuously distributed τ.

In the dashed-dotted curve in Fig. 5, it is clear that there are three distinct peaks. The values of τ (s) at the maxima and the corresponding integral values of $F^{(n)}(\tau)$ (C/cm^2) are (0.324, 1.03×10^{-5}), (11.0, 1.03×10^{-5}) and (331, 1.04×10^{-5}). Since the value of τ at the i-th maximum and the integral value of $F^{(n)}(\tau)$ correspond to τ_i and F_i, respectively, the values of τ_i and F_i are found to be close to the actual values.

On the other hand, it is easy to evaluate τ_i and F_i using eqs. (6) and (7), when it is considered that the dashed-dotted curve representing $S(t)$ in Fig. 4 results from the discrete F_i. In the dashed-dotted curve in Fig. 4, $t_{\mathrm{peak}i}$ (s) at the i-th peak and the corresponding peak value $S(t_{\mathrm{peak}i})$ [C/cm^2] are (0.324, 1.09×10^{-5}), (11.0, 1.09×10^{-5}) and (302, 1.00×10^{-5}). Since $\tau_i = t_{\mathrm{peak}i}$ and $F_i = S(t_{\mathrm{peak}i})$, the values of τ_i and F_i are found to be evaluated accurately.

In the above discussion, we have demonstrated how to evaluate $F(\tau)$ using $J_{\mathrm{dis}}(t)$. In the following section, individual cases are discussed.

3. Evaluation of Polarization and Relaxation Times of Dipoles

3.1 Dipoles with discrete relaxation times

A capacitor consisting of a dielectric film between two electrodes of unit area is considered. The time and temperature dependences of dipole polarization in the film are determined by competition between the orienting action of an electric field and the randomizing action of thermal motion. In the elementary theory of dielectrics,[16,18] the buildup of polarization $P_{\mathrm{p}i}(t_{\mathrm{cha}})$ in the capacitor during time t_{cha} after the application of a voltage V_{cha} at a temperature T is given by an exponential function of t_{cha}

$$P_{\mathrm{p}i}(t_{\mathrm{cha}}) = P_{\mathrm{s}i}\left[1 - \exp\left(-\frac{t_{\mathrm{cha}}}{\tau_i}\right)\right], \qquad (14)$$

where $P_{\mathrm{s}i}$ and τ_i are the steady-state polarization and relaxation time of the i-th dipole, respectively. Since the decay of polarization after removal of the applied voltage V_{cha} is expressed as

$$P(t) = \sum_i P_{\mathrm{p}i}(t_{\mathrm{cha}}) \exp\left(-\frac{t}{\tau_i}\right), \qquad (15)$$

the depolarization current density (i.e., transient discharge current density) $J_{\mathrm{dis}}(t)$ is given by

$$J_{\mathrm{dis}}(t) = -\frac{\mathrm{d}P(t)}{\mathrm{d}t} = \sum_i P_{\mathrm{p}i}(t_{\mathrm{cha}}) \frac{1}{\tau_i} \exp\left(-\frac{t}{\tau_i}\right). \qquad (16)$$

The values of $P_{\mathrm{p}i}(t_{\mathrm{cha}})$ and $P(t)$ correspond to F_i and $Q(t)$ in eqs. (2) and (3), respectively. Therefore, $P_{\mathrm{s}i}$ can easily be evaluated using eq. (14).

Let us consider a dielectric film with three kinds of dipoles; [τ_i (s), $P_{\mathrm{s}i}$ (C/cm^2)] = (0.3, 1×10^{-5}), (10, 1×10^{-5}) and (300, 1×10^{-5}). In the following, we demonstrate how to determine τ_i and $P_{\mathrm{s}i}$ more accurately, compared with the methods outlined in §2.2. The solid curve in Fig. 7 represents $S(t)$ for $t_{\mathrm{cha}} = 1000$ s. In the solid curve, $t_{\mathrm{peak}i}$ (s) and $S(t_{\mathrm{peak}i})$ (C/cm^2) are (0.326, 1.09×10^{-5}), (10.8, 1.09×10^{-5}) and (300, 9.64×10^{-6}). The values of τ_i and $P_{\mathrm{p}i}(1000)$ can be obtained using eqs. (6) and (7). However, the obtained values of τ_i ($i = 1, 2$) are greater than the actual values, because $S(t_{\mathrm{peak}i})$ is affected by the $(i+1)$-th dipole. In order to determine τ_1 and $P_{\mathrm{s}1}$ accurately, one must obtain $S(t)$ for $t_{\mathrm{cha}} = 0.326$ s (the first peak time in the solid curve), which is shown as the broken curve in Fig. 7. Since t_{peak1} is 0.302 s, τ_1 is 0.302 s. Since $S(t_{\mathrm{peak1}})$ is 6.65×10^{-6} C/cm^2, $P_{\mathrm{p}1}(0.326)$ is 6.65×10^{-6} C/cm^2 and then $P_{\mathrm{s}1}$ is evaluated as 1.01×10^{-5} C/cm^2 using eq. (14). Next, one must obtain $S(t)$ for $t_{\mathrm{cha}} = 10.8$ s (the second peak time in the solid curve) in order to evaluate τ_2 and $P_{\mathrm{s}2}$ accurately. This curve is shown as the dashed-dotted curve in Fig. 7. Since t_{peak2} and $S(t_{\mathrm{peak2}})$ in the dashed-dotted curve are 10.0 s and 6.64×10^{-6} C/cm^2, respectively, τ_2 and $P_{\mathrm{p}2}(10.8)$ are 10.0 s and 6.64×10^{-6} C/cm^2, respectively. Using eq. (14), $P_{\mathrm{s}2}$ is evaluated as 1.01×10^{-5} C/cm^2. In the solid curve, τ_3 and $P_{\mathrm{s}3}$ are evaluated to be 300 s and 1.00×10^{-5} C/cm^2, respectively. These evaluated values are almost equal to the actual values.

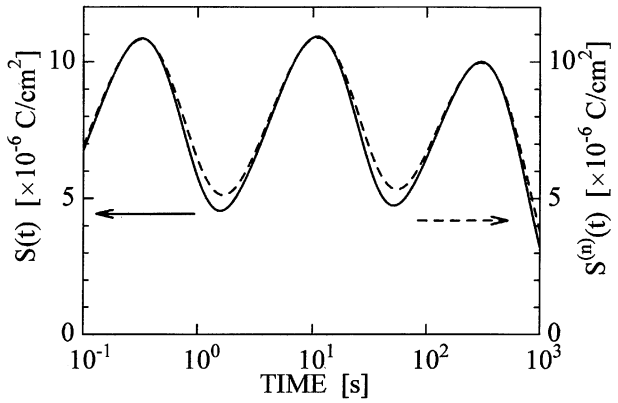

Fig. 6. $S(t)$ calculated using eq. (4) and $J_{\mathrm{dis}}(t)$ shown as the dashed-dotted curve in Fig. 2, and $S^{(n)}(t)$ calculated using eq. (10) and $F^{(n)}(\tau)$ shown as the dashed-dotted curve in Fig. 5.

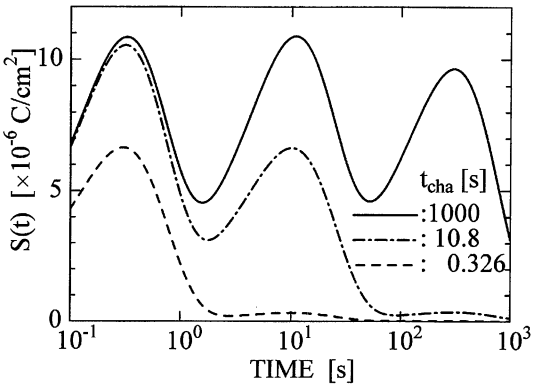

Fig. 7. Set of three kinds of $S(t)$ for three kinds of t_{cha}

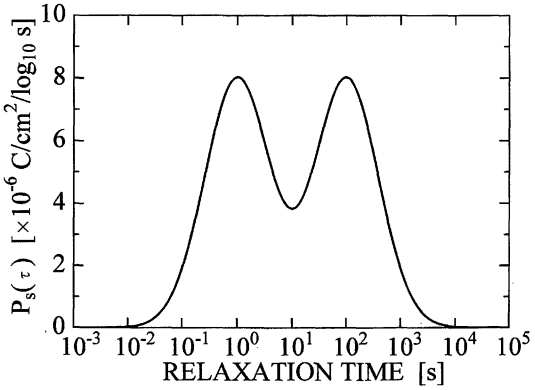

Fig. 8. Steady-state polarization $P_s(\tau)$.

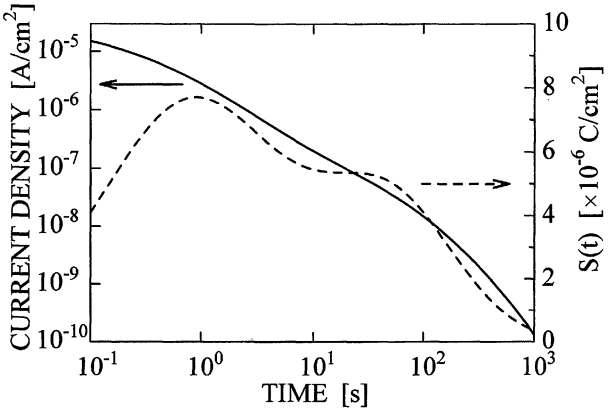

Fig. 9. $J_{dis}(t)$ and $S(t)$ for $t_{cha} = 100$ s in the capacitor with $P_s(\tau)$ shown in Fig. 8.

3.2 *Dipoles with continuously distributed relaxation time*

In the case of dipoles with continuously distributed τ, the buildup of polarization $P_p(\tau, t_{cha})$ in the capacitor during t_{cha} after the application of V_{cha} at T is given by an exponential function of t_{cha}

$$P_p(\tau, t_{cha}) = P_s(\tau)\left[1 - \exp\left(-\frac{t_{cha}}{\tau}\right)\right], \quad (17)$$

where $P_s(\tau)$ is the steady-state polarization corresponding to τ. Since the decay of polarization after removal of V_{cha} is expressed as

$$P(t) = \int P_p(\tau, t_{cha}) \exp\left(-\frac{t}{\tau}\right) d\tau, \quad (18)$$

$J_{dis}(t)$ is given by

$$J_{dis}(t) = -\frac{dP(t)}{dt} = \int P_p(\tau, t_{cha}) \frac{1}{\tau} \exp\left(-\frac{t}{\tau}\right) d\tau. \quad (19)$$

The values of $P_p(\tau, t_{cha})$ and $P(t)$ correspond to $F(\tau)$ and $Q(t)$ in eqs. (8) and (9), respectively. Therefore, $P_s(\tau)$ can easily be evaluated using eq. (17).

A dielectric film with the steady-state polarization $P_s(\tau)$ shown in Fig. 8 is considered. The solid and broken curves in Fig. 9 represent $J_{dis}(t)$ and $S(t)$ for $t_{cha} = 100$ s, respectively. Using the curve-fitting procedure outlined in §2, $P_p(\tau, t_{cha})$ shown as the solid curve in Fig. 10 is obtained. Using eq. (17), $P_s(\tau)$ shown as the broken curve

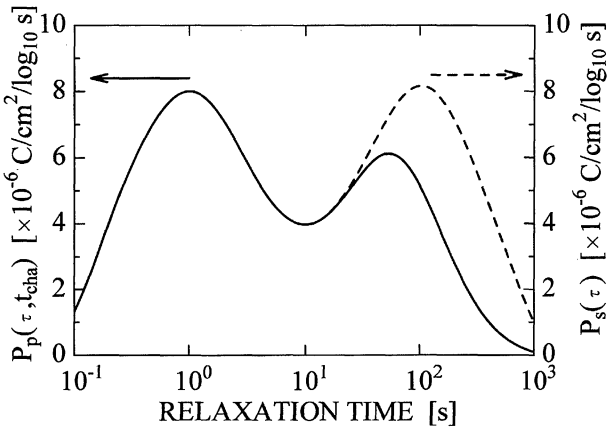

Fig. 10. $P_p(\tau, t_{cha})$ for which $S^{(n)}(t)$ approaches $S(t)$, shown in Fig. 9, very closely, and $P_s(\tau)$ calculated using eq. (17).

in Fig. 10 is obtained, which is quite similar to the actual $P_s(\tau)$ shown in Fig. 8.

Since $P_s(\tau)$ for a particular T and V_{cha} (i.e., electric field F_p) can be evaluated using this method, the dependence of $P_s(\tau)$ on T or F_p can be investigated in detail. As mentioned above, this method is suitable for the investigation of $P_s(\tau)$ in dielectrics (or ferroelectrics) with both discrete and continuously distributed τ.

4. Evaluation of Densities and Energy Levels of Traps

4.1 *Traps with discrete energy levels*

A capacitor consisting of a dielectric film between two electrodes of unit area is considered. The important parameters of traps in the film are the emission rate (e_t) from a trap and the trap density (N_t), where the relationship between e_t and τ is

$$e_t = \frac{1}{\tau}. \quad (20)$$

In order to simplify the following arguments, all traps are assumed to be filled with charged carriers when V_{cha} is applied to the capacitor in the interval of $-t_{cha} \leq t < 0$. The charge $Q_i(0)$ per unit area for the i-th trap level is expressed as

$$Q_i(0) = qN_{ti}, \quad (21)$$

where N_{ti} is the density of the i-th trap per unit area, and q is the magnitude of an electronic charge.

Since trapped carriers are emitted at $t > 0$, the charge $Q_i(t)$ in the film decreases with t according to

$$\frac{dQ_i(t)}{dt} = -e_{ti}Q_i(t), \quad (22)$$

where e_{ti} is the emission rate of the i-th trap. From eq. (22), $Q_i(t)$ is derived:

$$Q_i(t) = Q_i(0)\exp(-e_{ti}t). \quad (23)$$

Therefore, the total charge $Q(t)$ in the film of unit area is given by

$$Q(t) = \sum_i Q_i(t), \quad (24)$$

which is rewritten using eqs. (21) and (23) as

$$Q(t) = \sum_i qN_{ti} \exp(-e_{ti}t). \quad (25)$$

Since charged carriers, which are emitted from traps, are attributed to $J_{dis}(t)$,

$$J_{dis}(t) = -\frac{dQ(t)}{dt} = \sum_i qN_{ti}e_{ti} \exp(-e_{ti}t). \quad (26)$$

Comparing eq. (26) with eq. (3), qN_{ti} corresponds to F_i. Therefore, N_{ti} and e_{ti} can be obtained using $S(t)$ as

$$N_{ti} = \frac{S(t_{peaki})}{q} \quad (27)$$

and

$$e_{ti} = \frac{1}{t_{peaki}}. \quad (28)$$

4.2 Energetically distributed traps

In the case of energetically distributed traps, the charge $Q(0, e_t)$ captured by traps per unit area is expressed as

$$Q(0, e_t) = qN_t(e_t). \quad (29)$$

At $t > 0$, the charge $Q(t, e_t)$ in the film decreases with t according to

$$\frac{dQ(t, e_t)}{dt} = -e_tQ(t, e_t). \quad (30)$$

From eq. (30), $Q(t, e_t)$ is derived as

$$Q(t, e_t) = Q(0, e_t) \exp(-e_tt). \quad (31)$$

Since $\tau = 1/e_t$, the total charge $Q(t)$ in the film is given by

$$Q(t) = \int Q(t, e_t)d\left(\frac{1}{e_t}\right), \quad (32)$$

which is rewritten using eqs. (29) and (31) as

$$Q(t) = \int qN_t(e_t) \exp(-e_tt)\, d\left(\frac{1}{e_t}\right). \quad (33)$$

Since charged carriers, which are emitted from traps, are attributed to $J_{dis}(t)$,

$$J_{dis}(t) = -\frac{dQ(t)}{dt} = \int qN_t(e_t)e_t \exp(-e_tt)\, d\left(\frac{1}{e_t}\right). \quad (34)$$

Comparing eq. (34) with eq. (9), $qN_t(e_t)$ corresponds to $F(\tau)$. Therefore, $N_t(e_t)$ is obtained using $S(t)$.

4.3 Emission processes from traps

Since it is easy to investigate the temperature dependence of e_t using this method, it can be judged whether the carrier emission from traps is due to a tunneling process or to a thermal process. If $S(t)$ does not change with temperature, this emission probably is due to a tunneling process.

In the case of a thermal emission process, a trap level (ΔE_t) measured from the extended states can be evaluated. The emission rate e_t is given by[6,7,28]

$$e_t = \nu_t \exp\left(-\frac{q\Delta E_t}{kT}\right), \quad (35)$$

where ν_t is the attempt-to-escape frequency and k is the Boltzmann constant. Here, ν_t is given by $N_C v_{th} \sigma_t$, where σ_t is the cross section of traps, v_{th} is the thermal velocity of carriers, and N_C is the effective density of states in the extended states. Since v_{th} and N_C are proportional to $T^{1/2}$ and $T^{3/2}$, respectively, ν_t is expressed as

$$\nu_t = \nu_0 T^2, \quad (36)$$

where ν_0 is constant. Using the temperature dependence of e_{tpeak} corresponding to the peak of $S(t)$, ν_0 can be determined using the Arrhenius' plot [i.e., $\ln(e_{tpeak}/T^2) - 1/T$]. In consequence, the relationships

$$\Delta E_t = \frac{kT}{q} \ln\left(\frac{\nu_0 T^2}{e_t}\right) \quad \text{(eV)} \quad (37)$$

and

$$N_t(\Delta E_t) = N_t(e_t)\frac{q}{kT \ln 10} \quad (\text{cm}^{-2}\cdot\text{eV}^{-1}) \quad (38)$$

are obtained.[29]

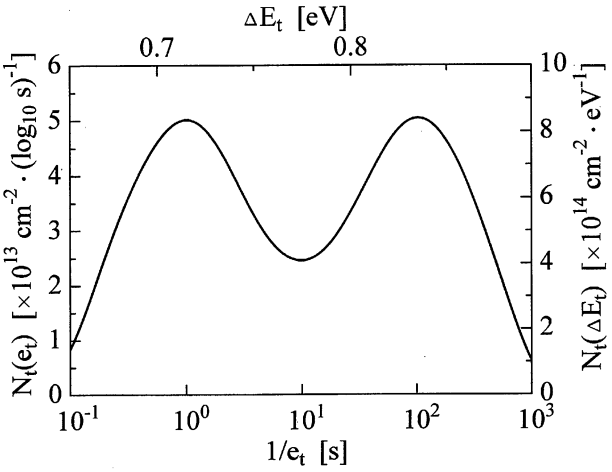

Fig. 11. $N_t(e_t)$ and $N_t(\Delta E_t)$ for $\nu_0 T^2 = 10^{12}\,s^{-1}$.

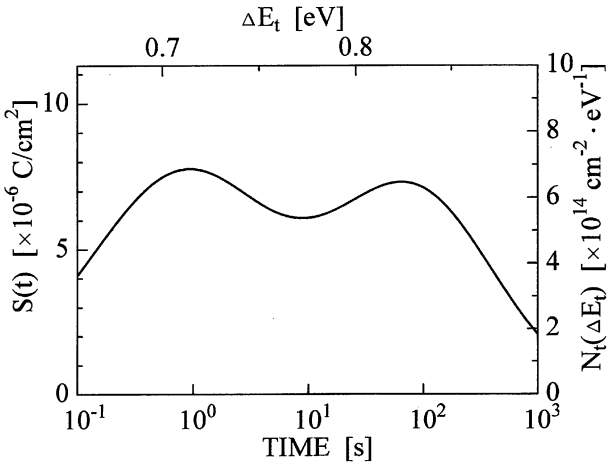

Fig. 12. $S(t)$ and $N_t(\Delta E_t)$ for $\nu_0 T^2 = 10^{12}\,s^{-1}$.

Figure 11 shows $N_t(e_t)$ and $N_t(\Delta E_t)$ for $\nu_0 T^2 = 10^{12}\,s^{-1}$, calculated using $S(t)$ shown as the broken curve in Fig. 4. Considering that $e_t = 1/\tau$ and $N_t(e_t) = F(\tau)/q$, the obtained $N_t(e_t)$ is quite similar to $F(\tau)$ shown as the broken curve in Fig. 3.

On the other hand, since $S(T)$ is rewritten as[29]

$$S(t) = \int qN_t(\Delta E_t)\exp(1)e_t t\exp(-e_t t)\mathrm{d}(\Delta E_t), \quad (39)$$

$N_t(\Delta E_t)$ is approximately given by[14]

$$N_t(\Delta E_t) \simeq \frac{S(t)}{kT\exp(1)} \quad (40)$$

and

$$\Delta E_t = \frac{kT}{q}\ln(\nu_0 T^2 t). \quad (41)$$

Using the above relationships, $S(t)$ shown as the broken curve in Fig. 4 can be converted to $N_t(\Delta E_t)$ for $\nu_0 T^2 = 10^{12}\,\mathrm{s}^{-1}$, which is shown in Fig. 12. The peaks of $N_t(\Delta E_t)$ in Fig. 12 are broader than the peaks of $N_t(\Delta E_t)$ in Fig. 11 because of the approximation in eq. (40). This analysis is useful for converting $S(t)$ into approximate $N_t(\Delta E_t)$.

5. Conclusions

We propose a simple graphical method for determining the polarization and relaxation times of dipoles and for determining the densities and emission rates of traps in a dielectric film using the transient discharge current of a capacitor which consists of the film between two electrodes. Since the values can be evaluated using the transient discharge current measured isothermally, it is unnecessary to assume the temperature dependence of time constants (i.e., relaxation times or emission rates) in order to analyze these data, suggesting that the temperature dependence of the time constants can be investigated in detail. When the transient discharge current arises from the thermal-emission of charged carriers from traps to the extended states, the energy levels of traps can be evaluated from the temperature dependence of emission rates. From the temperature dependence of time constants, it is possible to understand the origin of transient discharge currents, that is, depolarization of dipoles or carrier emission from traps (thermal emission process or tunneling process). Since many researchers are intending to make use of dielectrics or ferroelectrics as gate insulators in FETs and insulators of capacitors in DRAM, this method will play an important role in the investigation of dipoles and traps in these films.

1) E. Harari: J. Appl. Phys. **49** (1978) 2478.
2) P. Olivo, T. N. Nguyen and B. Ricco: IEEE Trans. Electron Devices **35** (1988) 2259.
3) D. V. Lang: J. Appl. Phys. **45** (1974) 3023.
4) H. Okushi and Y. Tokumaru: Jpn. J. Appl. Phys. **19** (1980) L335.
5) H. Okushi: Philos. Mag. B **52** (1985) 33.
6) H. Matsuura: J. Appl. Phys. **64** (1988) 1964.
7) H. Matsuura and H. Okushi: *Electrical Properties of Amorphous/Crystalline-Semiconductor Heterojunctions*, ed. J. Kanicki (Artech House, Boston, 1992) *Amorphous and Microcrystalline Semiconductor Devices*, Vol. II: Materials and Device Physics, Chap. 11.
8) N. M. Johnson, D. J. Bartelink and M. Schulz: *The Physics of SiO_2 and its Interfaces*, ed. S. T. Pantelides (Pergamon, New York, 1978) p. 421.
9) A. Ricksand and O. Engstrom: J. Appl. Phys. **70** (1991) 6915.
10) V. J. Kapoor and S. B. Bibyk: Thin Solid Films **78** (1981) 193.
11) B. H. Yun: Appl. Phys. Lett. **25** (1974) 340.
12) P. C. Arnett and B. H. Yun: Appl. Phys. Lett. **26** (1975) 94.
13) E. J. M. Kendall: Electron. Lett. **4** (1968) 468.
14) H. Matsuura, M. Yoshimoto and H. Matsunami: Jpn. J. Appl. Phys. **34** (1995) L185.
15) H. Matsuura, M. Yoshimoto and H. Matsunami: Jpn. J. Appl. Phys. **34** (1995) L371.
16) J. Vanderschueren and J. Gasiot: *Topics in Applied Physics: Thermally Stimulated Relaxation in Solids*, ed. P. Bräunlich (Springer-Verlag, Berlin, 1979) Vol. 37, Chap. 4.
17) H. Frei and G. Groetzinger: Phys. Z. **37** (1936) 720.
18) C. Bucci and R. Fieschi: Phys. Rev. Lett. **12** (1964) 16.
19) A. Servini and A. K. Jonscher: Thin Solid Films **3** (1969) 341.
20) J. G. Simmons and G. W. Taylor: Phys. Rev. B **6** (1972) 4804.
21) H. Matsuura: Jpn. J. Appl. Phys. **35** (1996) 2216.
22) H. Matsuura: Jpn. J. Appl. Phys. **35** (1996) 4711.
23) H. Matsuura and K. Sonoi: Jpn. J. Appl. Phys. **35** (1996) L555.
24) H. Matsuura: Jpn. J. Appl. Phys. **35** (1996) 5297.
25) H. Matsuura: Jpn. J. Appl. Phys. **35** (1996) 5680.
26) Since we consider $F(\tau)$ expressed in units of $\mathrm{C/cm^2/\log_{10} s}$, eq. (8) is rewritten as
$$Q(t) = \int F(\tau)\exp\left(-\frac{t}{\tau}\right)\mathrm{d}(\log_{10}\tau).$$
27) In order to obtain $F^{(n)}(\tau)$ as close to the actual $F(\tau)$ as possible, the definite integral with respect to $\log_{10}\tau$ of eq. (10) is calculated from $\log_{10}10^{-1}-1$ to $\log_{10}10^{3}+1$ on the assumption that $F^{(n)}(\tau) = F^{(n)}(10^{-1})$ in the range $10^{-2}\,\mathrm{s} \le \tau \le 10^{-1}\,\mathrm{s}$ and $F^{(n)}(\tau) = F^{(n)}(10^{3})$ in the range $10^{3}\,\mathrm{s} \le \tau \le 10^{4}\,\mathrm{s}$.
28) D. V. Lang, J. D. Cohen and J. P. Harbison: Phys. Rev. B **25** (1982) 5285.
29) When $N_t(e_t)$ is expressed in units of $\mathrm{1/cm^2/\log_{10} s}$, eq. (34) is rewritten as
$$J_{\mathrm{dis}}(t) = \int qN_t(e_t)e_t\exp(-e_t t)\,\mathrm{d}\left[\log_{10}\left(\frac{1}{e_t}\right)\right].$$
From eq. (37), the following relationship is obtained:
$$\mathrm{d}(\Delta E_t) = \frac{kT}{q}\cdot\ln 10\cdot\mathrm{d}\left[\log_{10}\left(\frac{1}{e_t}\right)\right].$$
Since $J_{\mathrm{dis}}(t)$ is rewritten as
$$J_{\mathrm{dis}}(t) = \int qN_t(e_t)e_t\exp(-e_t t)\mathrm{d}\left[\log_{10}\left(\frac{1}{e_t}\right)\right]$$
$$= \int qN_t(e_t)e_t\exp(-e_t t)\frac{q}{kT\ln 10}\mathrm{d}(\Delta E_t)$$
$$= \int qN_t(\Delta E_t)e_t\exp(-e_t t)\mathrm{d}(\Delta E_t),$$
the relationship expressed in eq. (38) is obtained:
$$N_t(\Delta E_t) = N_t(e_t)\frac{q}{kT\ln 10}.$$